Correlation of histopathology with magnetic resonance imaging in Kienböck disease

*Takeshi Ogawa M.D., Ph.D., **Yasumasa Nishiura M.D., Ph.D., **Yuki Hara M.D., Ph.D., ***Yoshikazu Okamoto M.D., Ph.D., **Naoyuki Ochiai M.D., Ph.D.

* Department of Orthopaedic Surgery, Kikkoman general hospital, 100 Miyazaki, Noda, Chiba, 278-0005, Japan

**Department of Orthopaedic Surgery, Graduate School of Comprehensive Human Sciences, University of Tsukuba, 1-1-1 Tennodai, Tsukuba, Ibaraki, 305-8575, Japan

*** Department of Radiology, Graduate School of Comprehensive Human Sciences, University of Tsukuba, 1-1-1 Tennodai, Tsukuba, Ibaraki, 305-8575, Japan

Corresponding author: Takeshi Ogawa, M.D. Ph.D.

Department of Orthopaedic Surgery, Kikkoman general hospital, 100 Miyazaki, Noda-shi, Chiba 278-0005, Japan

Tel: +81-4-7123-5911. Fax: +81-4-7123-5920.

E-mail address: oga-take@pg7.so-net.ne.jp

【A running title】

Correlation of histopathology with MRI in Kienböck disease

【Key words】

Kienböck disease, histopathology, magnetic resonance imaging, lunate, bone necrosis

【Acknowledgement】

The authors thank Masayuki Noguchi, M.D., Ph.D. (Department of Pathology, Institute of Basic Medical Science, Graduate School of Comprehensive Human Science, University of Tsukuba, Tsukuba, Ibaraki, Japan) for the technical assistance and good advice for pathology.

Introduction

The treatment of Kienböck disease remains controversial; however, it is agreed that early diagnosis is important.[1-3] Magnetic resonance imaging (MRI) of Kienböck disease typically gives a uniformly low signal on T1-weighted images. MRI is essential for an early diagnosis.[4, 5] However, it is difficult to understand the detail of the actual histology, which can enable the selection of appropriate treatment options. Few reports have correlated MRI scans and histopathological appearances of biopsy specimens[6, 7] or comparisons with sagittal sections of whole lunate bones.[8] As compared to the histological findings, low-intensity areas on MRI did not correlate closely with the extent of the necrotic areas and did not distinguish between new bone formation and granulation tissue. Moreover, Hashizume et al. said that this disagreement was due to the poor quality of the MRI.[8] Schmitt et al. summarized the pathoanatomic processes and the corresponding MRI findings in the natural course of lunate osteonecrosis.[9] In close correlation with the underlying pathoanatomic processes, 3 different signal and contrast enhancement patterns can be identified in lunate osteonecrosis with the use of contrast-enhanced, T1-weighted MRI. This imaging technique clearly shows the different enhancement patterns and differentiation between bone marrow edema and partial and complete bone marrow necrosis.[9,10]

The purpose of this study was to compare in the detail pre-surgery MRI scans with the corresponding coronal sections of extirpated lunates of patients with Kienböck disease. Our hypothesis is that the MRI scans taken with 47-mm microscopy surface coil are reflected the histopathology of Kienböck disease.

Materials and methods

Six patients (3 men and 3 women; aged 21–64 years; average 38 years) with Kienböck

52 disease underwent tendon-ball replacement[11] or the Graner surgical procedure (lunate
53 excision, capitate osteotomy, and intercarpal arthrodesis)[12,13] between 2005 and 2008 at
54 our Hospital. Each patient was examined by radiography and MRI. Lichtman's criteria
55 were used to identify stage 3b Kienböck disease on the x-ray.
56 MRI was performed within 1 month before surgery using a 1.5-T system (Gyroscan NT
57 Intera; Phillips Medical Systems, Best, The Netherlands). Coronal 2-dimensional
58 proton-density weighted (PDW) (T1-weighted) (repetition time [TR][msec]/echo time
59 [TE][msec] = 1697-1852/17.0) images, and fast-field echo (FFE)(T2-weighted) (TR/TE
60 = 392-396/13.8-14.0) images of the wrist were acquired using a 47-mm microscopy
61 surface coil (Philips Medical Systems, Best, The Netherlands). The microscopy coil is
62 intended for a range of applications requiring a small field of view while maintaining a
63 high signal-to-noise ratio and is well suited to exame small anatomical lesions. The slice
64 thickness was 1.5-mm, and the slice interval was 0.1-mm with a field of view of
65 50-mm.[14,15] Under these conditions, the lunate bones were imaged in 8 slices of the
66 coronal view. A radiologist (Y.O.) and the author (T.O.) observed all preparations and
67 evaluated the images.
68 The whole lunate bones were extirpated during replacement surgery and were fixed in
69 a 10% buffered neutral formalin solution (Wako®, Osaka, Japan). After decalcification
70 in 0.5 M EDTA, 0.1 M Tris and NaOH for 4 months, the samples were embedded in
71 paraffin. The decalcified whole lunates were sectioned roughly into 8 coronal specimens
72 (Fig. 1) correlating with the coronal MRI and were stained with hematoxylin-eosin.
73 Given that a long axis of the lunate was about 20mm, the width of 8 coronal specimens
74 was about 2mm. Since the slice thickness of MRI was 1.5mm, the error was presumed to
75 be up to about 1mm.

Assessment points of histopathological osteonecrosis included observations of empty lacunae, fatty marrow, and vascular structures, and the findings were compared with the signal levels of the PDW- and FFE-coronal MRI at the same slice levels. The author (T.O.) and another researcher (Y.H.) familiar with histopathological evaluations made the histological observations of the slices. In total, 8 views from the MRI and 8 slices of the histopathological specimens that were similar in shape macroscopically were compared by the author (T.O.) with regards to the assessment points of histopathological osteonecrosis.

Results

Generally, PDW images of normal lunates exhibit high signal intensities, whereas FFE images exhibit intermediate intensities.[7] In comparison, the PDW images of the necrotic lunate in this study demonstrated lower signal intensities, and the FFE images exhibited higher or lower intensities .[16] The overall MRI and histopathological observations of each diseased lunate are shown in Table 1. Sagittal diagrams include images taken from the central part of the coronal view (Fig. 2). Histopathological analyses revealed disrupted trabecular and degraded fatty marrows towards the center of the lunates. However, on the dorsal and palmar aspects of the lunates, the trabecular structures, fatty marrows, and blood vessels appeared normal. Likewise, the palmar and dorsal aspects of the lunates maintained near-normal intensities as observed in the PDW images.

The pre-surgical MRI and histopathological images of a representative case are shown Figure 3. Towards the center of the lunate, the signal intensity of the PDW images was reduced, and segmented trabecular structures were observed in the corresponding

histopathological views. The details of a representative slice level are shown (Fig. 3c, k, s). Within the solid outline (Fig. 4, upper row), the region appeared nearly normal histopathologically because we could observe trabecular structures and fatty marrow (Fig. 4a). This region also exhibited high intensity PDW images and moderate intensity FFE images. Furthermore, the observed signal was equal to the signal of the normal osseous tissue in the MRI. Conversely, within the dotted outline (Fig. 4, upper row), the region was filled with fibrous granular tissue and blood vessels, and no fatty marrow or osteocyte nuclei were observed histopathologically (Fig. 4b). This region also exhibited slightly low intensity PDW images and high intensity FFE images. In all specimens, we observed a signal change on the MRI, as well as changes in the histopathology. In the dorsal distal region (Fig. 3a, i, q), near-normal signal intensities were observed on the MRI, and normal trabecular structures were observed in the histopathological analyses, including osteocyte nuclei, fatty marrow, and blood vessels. This region also exhibited high intensity PDW images and intermediate intensity FFE images (Fig. 3a, i, q). In the volar 1/3 area (Fig. 3f, n, v) of the lunate, there were fibrous granular tissues and blood vessels but an absence of fatty marrow, and this area exhibited low intensity PDW images and high intensity FFE images.

Of the 6 patients having Kienböck disease (stage 3b), osteocyte nuclei, fatty marrow, and blood vessels were present within the corresponding high intensity areas of the PDW images. In the low intensity areas of the PDWs, osteocyte nuclei and fatty marrow were absent, and blood vessels were only present in some of the histopathological findings. The intensities of the FFE images and the histopathological findings did not always correlate (Table 2).

Discussion

In normal bone, T1-weighted MRI images have a high signal, and T2-weighted MRI images show an intermediate signal. However, in the early stages of osteonecrosis, T1-weighted images exhibit a low signal, and T2-weighted images show a high signal. This intensity change reflects a loss of fatty marrow affecting the T1 signal and possible edema contributing to a high signal in the T2-weighted images. In the more advanced stages of osteonecrosis, T1- and T2-weighted images both show low signal intensities .[16] In the present cases, the lunate conditions were assumed to be advanced osteonecrosis because of stage 3b on x-ray; however, the MRI scans using a 47-mm microscopy coil showed a variety of focal changes.

Desser et al. (1990) showed that MRI was able to distinguish areas of viable and nonviable bone within the lunate. They further demonstrated that undecalcified, fluorescently-labeled histological sections of lunate biopsies exhibited tetracycline uptake.[7] Trumble et al. (1990) showed that 6 patients having a diagnosis of Kienböck disease demonstrated a correlation between the loss of signal intensity on T1- and T2-weighted MRI images and evidence of osteonecrosis by histology. However, the extent of marrow changes that must be present for signal intensity alterations in MRI scans has not been determined.[6] Hashizume et al. (1996) histologically examined extracted whole lunates from 10 patients with Kienböck disease (stage 3). All of the patients showed a markedly decreased intensity of the lunate on MRI in sagittal T1-weighted images. In T2-weighted images, 2 cases showed complete low intensity, and 3 cases yielded diffuse images that included mixed high and low areas. MRI (T1- and T2-weighted images) low-intensity areas did not correlate closely with the extent of the necrotic areas in the histological findings and did not distinguish between new bone

148 formation and granulation tissue in detail. Moreover, they said that this disagreement
149 was due to the poor quality of the MR images.[8] In our 6 cases, empty lacunae and a
150 reduction of fatty marrow, but not the presence of blood vessels, correlated with the
151 signal intensities of the PDW images taken with a 47-mm microscopy coil.
152 Kienböck disease is denoted as an avascular necrosis because blood vessels are usually
153 not present. In the lunates of our study, the trabecular bone structures were segmented,
154 and fatty marrows were absent, which potentially allowed the formation of fibrous
155 granulation tissues, although with the presence of blood vessels. Hashizume et al.
156 (1996) reported that necrotic areas were invaded with new bone formation and
157 granulation. The necrotic tissue then changed into fibrous scar tissue and necrotic
158 debris. Around the necrotic area, non-necrotic tissues under hypervascularized
159 conditions were reactive to the necrosis.[8] Even if there are blood vessels
160 histopathologically, it is unknown whether there is effective blood flow or interosseous
161 pressure when evaluated by MRI. If we can know the effective blood flow in the lunate,
162 it may be useful for selecting treatment or elucidating the etiology of Kienböck disease.
163 Schmitt et al. (2007) classified 3 patterns for Kienböck disease by using
164 contrast-enhanced MRI and described this classification as the best evaluation for the
165 viability of bone marrow.[9] Certainly, to evaluate blood flow and the bone marrow edema
166 of the lunate in detail, gadolinium enhanced MRI is necessary.
167 The absence of gadolinium enhancement in our study is a limitation. Additional
168 limitations include the small number of cases, low field strength, and minimal imaging
169 conditions.
170

References

1. Beredjiklian PK. Kienbock's disease. J Hand Surg 2009; 34A:167-175.
2. Innes L, Strauch RJ. Systematic review of the treatment of Kienbock's disease in its early and late stages. J Hand Surg Am 2010; 35:713-7, 17 e1-4.
3. Squitieri L, Petruska E, Chung KC. Publication bias in Kienbock's disease: systematic review. J Hand Surg Am 2010; 35:359-367 e5.
4. Amadio PC, Hanssen A D, Berquist TH. The genesis of Kienbock's disease: evaluation of a case by magnetic resonance imaging. J Hand Surg Am 1987; 12:1044-1049.
5. Imaeda T, Nakamura R, Miura T, Makino N. Magnetic resonance imaging in Kienbock's disease. J Hand Surg Br 1992; 17:12-19.
6. Trumble TE, Irving J. Histologic and magnetic resonance imaging correlations in Kienbock's disease. J Hand Surg Am 1990; 15:879-884.
7. Desser TS, McCarthy S, Trumble T. Scaphoid fractures and Kienbock's disease of the lunate: MR imaging with histopathologic correlation. Magn Reson Imaging 1990; 8:357-361.
8. Hashizume H, Asahara H, Nishida K, Inoue H, Konishiike T. Histopathology of Kienbock's disease. Correlation with magnetic resonance and other imaging techniques. J Hand Surg Br 1996; 21:89-93.
9. Schmitt R, Krimmer H. Osteonecrosis of the hand skeleton. In: Schmitt R, Lanz U, eds. Diagnostic Imaging of the Hand. 1st end. Stuttgart, New York: Georg Thieme Verlag; 2007; 351-364.
10. Schmitt R, Christopoulos G, Kalb K, Coblenz G, Frohner S, Brunner H, Krimmer H, Lanz U. Differential diagnosis of the signal-compromised lunate in

MRI. Rofo 2005; 17: 358-366.

11. Ueba Y, Nosaka K, Seto Y, Ikeda N, Nakamura T. An operative procedure for advanced Kienbock's disease. Excision of the lunate and subsequent replacement with a tendon-ball implant. J Orthop Sci 1999; 4:207-215.

12. Graner O, Lopes EI, Carvalho BC, Atlas S. Arthrodesis of the carpal bones in the treatment of Kienbock's disease, painful ununited fractures of the navicular and lunate bones with avascular necrosis, and old fracture-dislocations of carpal bones. J Bone Joint Surg Am 1966; 48: 767-774.

13. Takase K, Imakiire A. Lunate excision, capitate osteotomy, and intercarpal arthrodesis for advanced Kienbock disease. Long-term follow-up. J Bone Joint Surg Am 2001; 83: 177-183.

14. Tanaka T, Yoshioka H, Ueno T, Shindo M, Ochiai N. Comparison between high-resolution MRI with a microscopy coil and arthroscopy in triangular fibrocartilage complex injury. J Hand Surg Am 2006; 31: 1308-1314.

15. Yoshioka H, Ueno T, Tanaka T, Kujiraoka Y, Shindo M, Takahashi N, Nishiura Y, Ochiai N, Saida Y. High-resolution MR imaging of the elbow using a microscopy surface coil and a clinical 1.5 T MR machine: preliminary results. Skeletal Radiol 2004; 33: 265-271.

16. Schmitt R, Heinze A, Fellner F, Obletter N, Struhn R, Bautz W. Imaging and staging of avascular osteonecroses at the wrist and hand. Eur J Radiol 1997; 25: 92-103.

Figure legends

Figure 1. Whole lunate with a schema of the 8 coronal slices scanned using MRI.

Figure 2. MRI analysis of each patient. Sagittal diagrams include images taken from the central part of the coronal view.

Figure 3. Pre-surgical PDW images (a–h) and FFE images (i–p) and HE stained sections (q–x) (x 12.5) taken from the dorsal to palmar side of the lunate from a 21-year-old left-handed woman that underwent a Graner surgical procedure for Kienböck disease (stage 3b).

Figure 4. Representative slice levels (taken from Fig. 2c, k, s) and correlating histology. Within the solid outline (upper row), the region appeared nearly normal histopathologically because we could observe trabecular structures and fatty marrow (a). This region also exhibited high intensity PDW images and moderate intensity FFE images and was equal to the signal of the normal osseous tissue in the MRI. Conversely, within the dotted outline (upper row), this region contained fibrous granular tissue and blood vessels, and no fatty marrow or osteocyte nuclei were observed histopathologically (b). (a) A high magnification image of the squared encircled area in (c, k and s). Osteocyte nuclei, fatty marrow, and blood vessels are present within the vitalized focal area of the solid line. (b) Fibrous granular tissues and blood vessels are present, whereas there is an absence of fatty marrow within the dotted line.

Table 1. MRI and histopathological analysis of each patient.

Table 2. Correlation of the histopathology with the MRI scans: (+), presence; (±), discordance; (-), absence.

241 Figure 1.

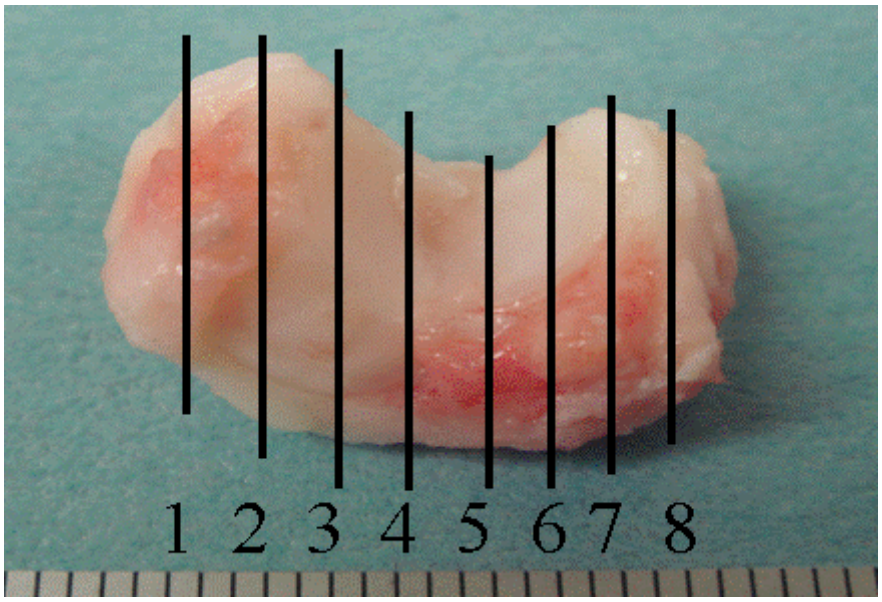

242

243

244 Figure 2.

245

246

Patient	*MRI finding*			
	PDW		*FFE*	
		sagittal diagram		*sagittal diagram*
1	normal or partial slightly low (dorsal 1/3 and volar 1/3), low (central 1/3)	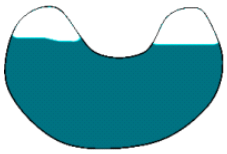	normal (dorsal 1/3 and volar 1/4), low (another central part)	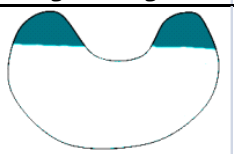
2	normal (dorsal1/2), low (volar1/2)		normal (dorsal1/2), low (volar1/2)	
3	normal (dorsal1/4 and volar-ulnar sides), low(dorsal 1/4 to volar-radial sides)	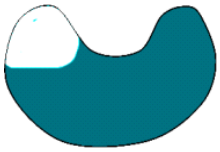	high (dorsal1/3 and volar-ulnar sides), low (dorsal 1/3 to volar-radial sides)	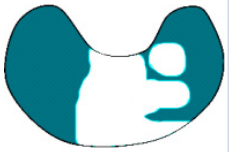
4	all slices are slightly low	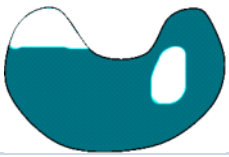	all slices are high and low (diffuse or partial)	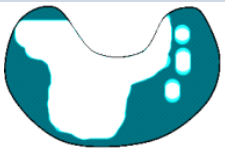
5	low (volar1/4), another slices are slightly low	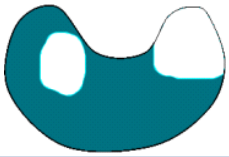	normal (dorsal 1/3), high(diffuse or partial)(center to volar side)	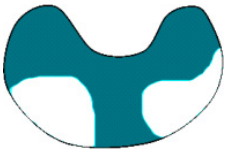
6	normal or partially slight low (dorsal 1/3 and volar 1/3), low (central 1/3)	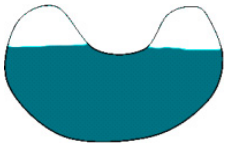	high (dorsal3/4), normal (volar 1/4)	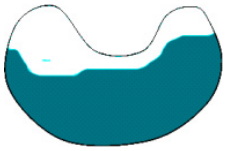
Normal	hyperintense signal	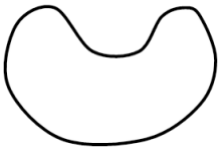	intermediate signal	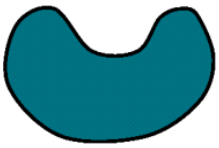

247 Figure 3.

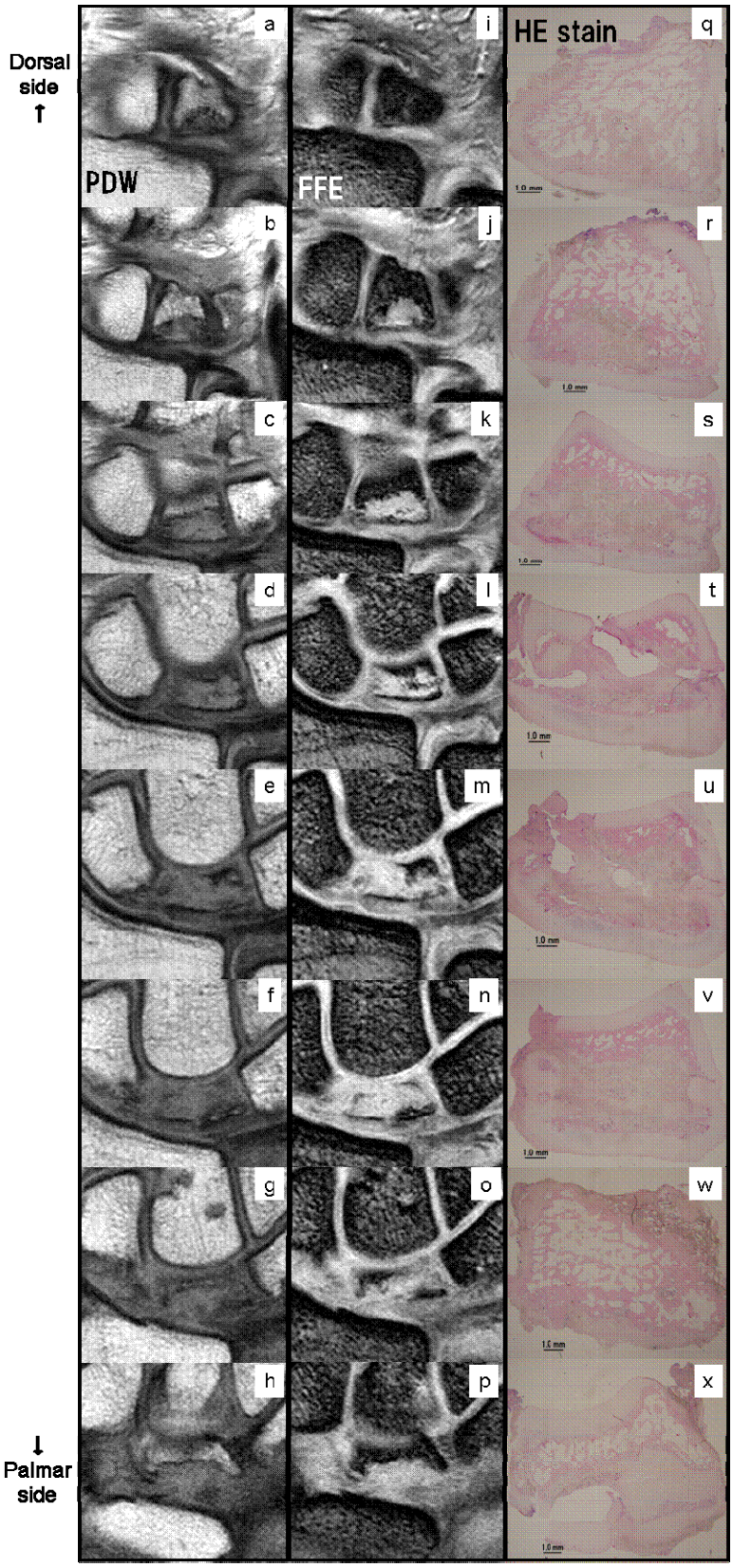

248

249

250 Figure 4.

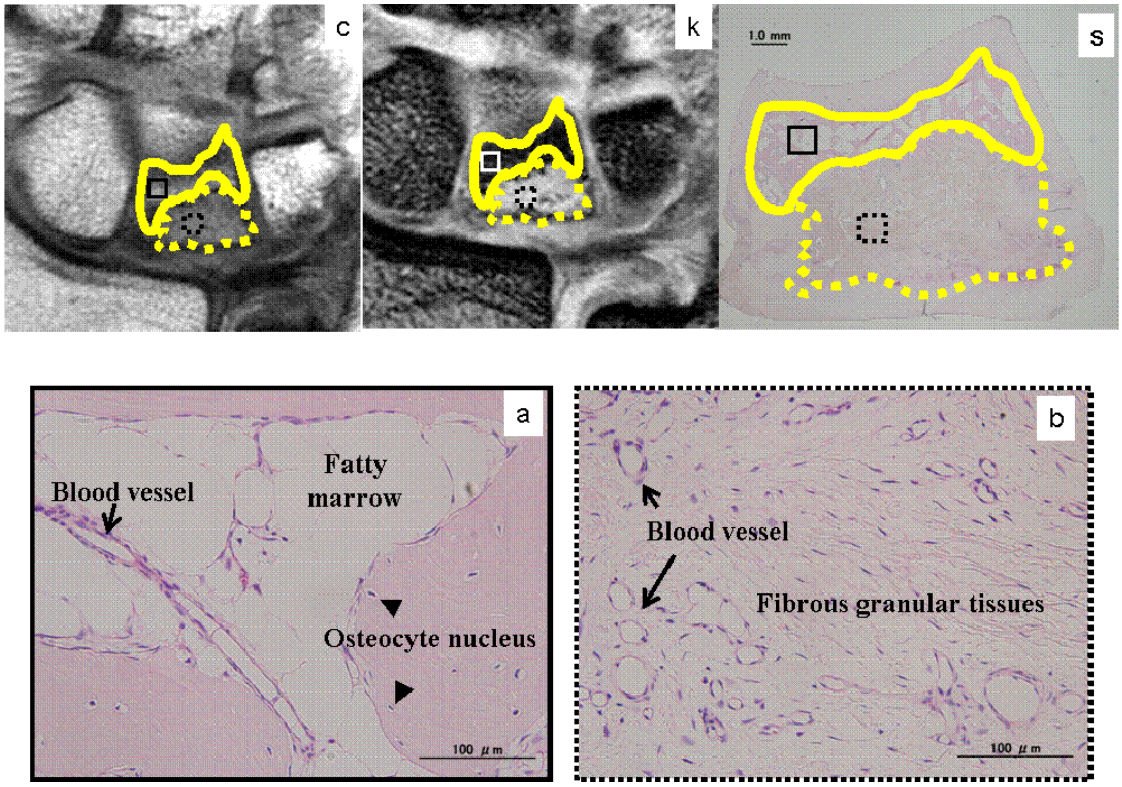

251

252

253 Table 1.

Patient	*Gender*	*Age*	*X-ray finding*	*Histopathlogical finding*			*MRI finding*	
				Empty lacunae	*Fatty marrow*	*Blood vessel*	*PDW*	*FFE*
1	F	65	segmentation and comminuted fracture at central 1/3	partially presence (central 1/3), a few (dorsal 1/3 and volar 1/3)	absence (central 1/3), partially presence (dorsal 1/3 and volar 1/3)	partially presence in all slices	normal or partial slightly low (dorsal 1/3 and volar 1/3), low (central 1/3)	normal (dorsal 1/3 and volar 1/4), low (another central part)
2	M	24	segmentation at volar 1/3	presence (dorsal1/3), absence (volar2/3)	presence (dorsal1/3), absence (volar2/3)	presence (dorsal1/3), absence (volar2/3)	normal (dorsal1/2), low (volar1/2)	normal (dorsal1/2), low (volar1/2)
3	M	21	severe collapse, especially radial side	partially presence in all slices	partial presence (dorsal1/4 and volar–ulnar side)	partially presence in all slices	normal (dorsal1/4 and volar–ulnar sides), low(dorsal 1/4 to volar–radial sides)	high (dorsal1/3 and volar–ulnar sides), low (dorsal 1/3 to volar–radial sides)
4	M	33	segmentation(+) colonal and sagittal plane on center	partially presence in all slices	partially presence (dorsal 1/3) , absence (central to volar 1/3)	partially presence in all slices	all slices are slightly low	all slices are high and low (diffuse or partial)
5	F	64	segmentation at volar 1/3	presence (dorsal2/3), absence (volar1/3)	absence in all slices	dorsal2/3 is absence, volar1/3 is presence	low (volar1/4), another slices are slightly low	normal (dorsal 1/3), high(diffuse or partial)(center to volar side)
6	F	21	segmentation and comminuted fracture at volar 1/3	partially presence (central 1/3), a few (dorsal 1/3 and volar 1/3)	absence (central 1/3), partially presence (dorsal 1/3 and volar 1/3)	partially presence in all slices	normal or partially slight low (dorsal 1/3 and volar 1/3), low (central 1/3)	high (dorsal3/4), normal (volar 1/4)
Normal			screlotic change (–) collapse (–) segmentation(+)	absence	presence	presence	hyperintense signal	intermediate signal

254

255

256 Table 2.

257

MRI finding		Histopathological finding			osteonecrosis
		Osteocyte nucleus	Fatty marrow	Blood vessel	
PDW image	intermediate	+	+	+	-
	slightly low	-	-	±	+
	low	-	-	±	+
FFE image	high	±	±	±	±
	intermediate	+	+	+	-
	low	±	±	±	±

258

259

Abstract

Purpose Diagnosis and treatment remain controversial for Kienböck disease. A few reports have correlated magnetic resonance imaging (MRI), which is essential for early diagnosis, and histopathology of Kienböck biopsy specimens, but histopathological correlations of whole lunate bones or histological slices compared with MRI images are lacking. The purpose of this study was to compare pre-surgical MRI scans taken with a 47-mm microscopy surface coil with corresponding histological slices of Kienböck diseased lunates.

Materials and methods Extirpated whole lunates were harvested at the time of surgery from 6 patients with Kienböck disease (stage 3b) undergoing tendon-ball replacement or a Graner surgical procedure. Paraffin-embedded, coronally sectioned specimens were stained with hematoxylin-eosin and compared with pre-surgical coronal scans using MRI with a 47-mm microscopy surface coil.

Results Towards the center of the lunates, the signal intensity in the proton-density weighted (PDW) images was reduced, whereas the dorsal and palmar sides of the lunates exhibited no changes in intensity. In correlation, histopathological findings revealed strongly disrupted trabeculae toward the center of the lunates and intact trabeculae in the dorsal side of the lunates. Likewise, the necrotic and vitalized bone exhibited low and high signal intensities, respectively, in the PDW images; however, in the fast-field echo (FFE) images, there were no correlations with the histopathological observations.

Conclusions MRI (PDW images, but not FFE images) using a 47-mm microscopy coil reflected the extent and localization of the necrotic area in Kienböck diseased lunates, as evidenced by comparison with histological analyses of the lunate specimens.